v. 3, n. 41, 2023

Journal of Engineering Research

EFFECTS OF THE SOLIDIFICATION SEQUENCE ON THE DISTRIBUTION AND MORPHOLOGY OF THE PRIMARY EPSILON PHASE IN ZN-(3-4)AL-(3.8-5.6)CU ALLOYS

Eduardo Daniel Jareño Betancourt
``Universidad Autónoma de Zacatecas``, Zacatecas, Mexico
https://orcid.org/0000-0001-9624-439X

Salvador Gómez Jiménez
``Universidad Autónoma de Zacatecas``, Zacatecas, Mexico
http://orcid.org/0000-0001-6654-3313

Abstract: The solidification sequence influences the formation and growth of phases in a metal alloy. In Zn-(3-4)Al-(5-10)Cu alloys, the epsilon phase determines their mechanical properties. Previous research has analyzed the effect of Cu content and solidification kinetics on this phase. In this study, using thermal analysis and optical microscopy techniques, the effect on the microstructure of cooling rates at different positions with respect to the solidification front was observed by tempering the alloy from the formation temperature of the primary phase after applying different thermal cycles.
Keywords: Zn-Al-Cu alloys, epsilon phase, cooling rate, solidification front.

INTRODUCTION

The formation, growth and morphology of the epsilon phase has been related to the mechanical properties of Zn3-27Al5-10Cu alloys (Durman, 1991-1997; Rashid, 1991; Hanna, 1997). An important part of the research on these alloys includes this phase. Durman and Murphy (1991) concluded that the increase in the mechanical properties of ZA8 alloys is due to the formation of epsilon phase precipitates in the eta phase matrix. Rashid and Hanna (1991, 1997) in their patents describe the epsilon ratio with the other phases and its effect on the mechanical properties in Zn3Al(5-10)Cu (ACuZinc) alloys. In another investigation, the growth rate is related to the epsilon phase fraction and morphology in Zn-rich Zn-Cu alloys (Ma, 2000). The author of the present study published his results on the effect of cooling conditions on the fraction and morphology of this phase in Zn-Al-Cu alloys (Jareño et. Al, 2010). Some of the aforementioned results could be considered contradictory if the experimental procedures with which they were obtained are not taken into account. The superheat temperature, the permanence at high temperatures, the cooling rate and other metallurgical and process parameters affect the microstructure of the cast metal alloys (Lazkari, 2007). In this sense, taking as reference the solidification conditions in which some of the aforementioned results were obtained, an experimental procedure was developed that has allowed us to observe how the epsilon phase behaves under different solidification sequences.

EXPERIMENTAL PROCEDURE

Two experimental alloys and one commercial alloy were used. The chemical composition was verified by atomic absorption spectrometry. The first with a weight percentage of 4.54Cu, 3.9Al, 0.3Mg (denoted 4.5Cu) and the second with 3.83Cu, 4Al, 0.3Mg (3.8Cu), balance, Zn and impurities. The ACuZinc5 commercial alloy used is within the ASTM B892 standard: 5.58Cu, 3.18Al, 0.04Mg. To vary the sequence and solidification conditions of the experimental alloys, two thermal cycles were used in two different graphite cups. For Thermal Cycle I (CTI), in the cup presented in Fig. 1, three samples of the 4.5Cu alloy were heated approximately 10 °C above the start temperature of the primary reaction (426 °C, formation of the primary phase epsilon, ε) and then quenched in water at 7 °C. For Thermal Cycle II (CTII), the graphite cup in Fig. 2 was used and 3 samples of each alloy were heated 10 °C above the primary reaction temperature (3.8Cu, 409 °C, formation of the primary phase epsilon, ε) then the temperature was decreased by 10 °C, remaining there for 30 minutes to finish quenching in water at 7 °C.

In the case of the commercial alloy ACuZinc 5 and the experimental alloy 4.5 Cu, a third thermal cycle (CTIII) was applied to them that included mechanical stirring during solidification, Fig. 3. The temperatures that appear on the line are those corresponding to the commercial alloy ACuZinc5 and

the temperatures in parentheses to the experimental alloy 4.5Cu. In this thermal cycle, a first isothermal plateau was carried out for homogenization, approximately 20 °C above the formation temperature of the primary phase epsilon, ε, followed by gradually decreasing the temperature until the end temperature of the primary reaction and Start stirring at 250 rpm for an isothermal stay for 10 minutes. At the end, the alloy is suddenly cooled to observe the result of the applied procedure. For sudden cooling, the sample was poured onto a 3 mm thick AISI 304 stainless steel surface cooled in advance from the bottom with water at 8 °C. The casting surface was limited by a square of 40 mm side by 6 mm height of the same material as the casting surface. The reaction temperatures used were determined in a previous study (Jareño, 2010).

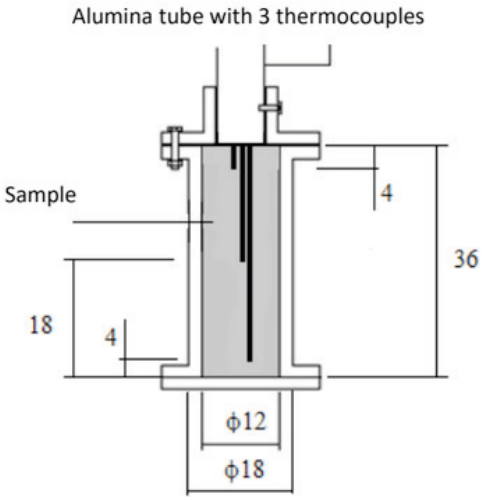

Fig. 1 Graphite cup for CTI

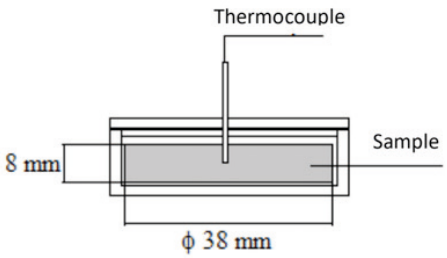

Fig. 2 Graphite cup for CTII

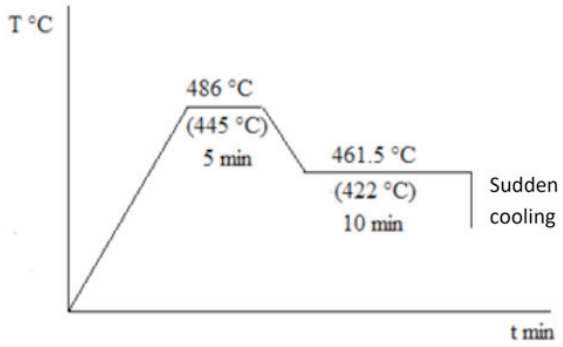

Fig. 3 Thermal cycle CTIII with mechanical agitation

MICROSTRUCTURAL ANALYSIS

The samples obtained using the graphite cup shown in Fig. 1 were cross-sectioned through the tip of each thermocouple with the objective of observing the microstructure corresponding to the cooling curve obtained from the data of the temperature variation over time. CTI product. In the case of the cup shown in Fig. 2, it was sectioned parallel to the thermocouple in a longitudinal direction. The samples obtained through the CTIII thermal cycle, Fig. 3, were sectioned as represented in Fig. 4. The polished samples were etched with the Tinofeef reagent (Haughton, 1921) and the photomicrographs were obtained with an Olympus Vanus AHMT3 optical microscope.

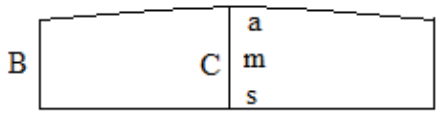

Fig. 4 Sectioning of the sample and identification of the study areas

DISCUSSION OF RESULTS

Fig. 5 shows a graph with the cooling curves obtained during the quenching of the 4.5Cu alloy after applying the CTI thermal cycle. The curve obtained with the readings on the thermocouple whose tip is at the top of the sample according to Fig. 1, Tm in the middle part and Tf at the bottom is called Ta. The curves corresponding to the thermocouples

placed in the middle and above the sample have a similar behavior, while the Tf curve of the thermocouple close to where the contact with the cold water begins, indicates that in that area the sample solidifies around the half the time if we consider that the end of solidification temperature for this alloy is approximately 370 °C (Jareño, 2010).

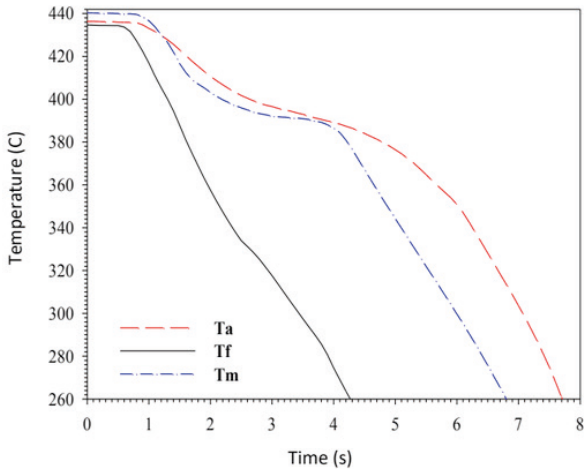

Fig. 5 Rapid cooling curves obtained by thermal analysis using three thermocouples, Fig. 1

If parallel to this, the photomicrographs contained in Figs. 6a and 6b corresponding to the Ta and Tm curves in Fig. 5, we note that their microstructure is similar, this is not the case in Fig. 6c where a different distribution and morphology of the phases that make up the microstructure related to the Tf curve is observed.

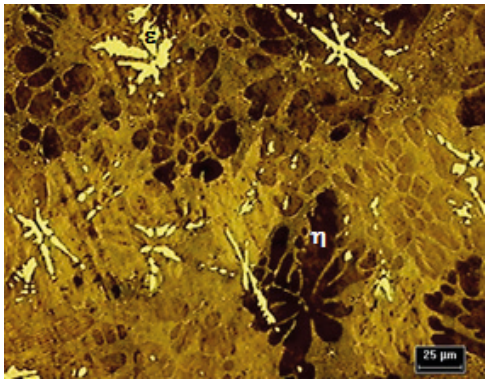

Fig. 6a Top of the sample (Ta)

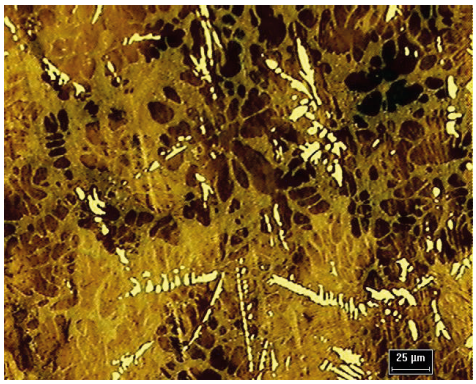

Fig. 6b Middle part of the sample (Tm)

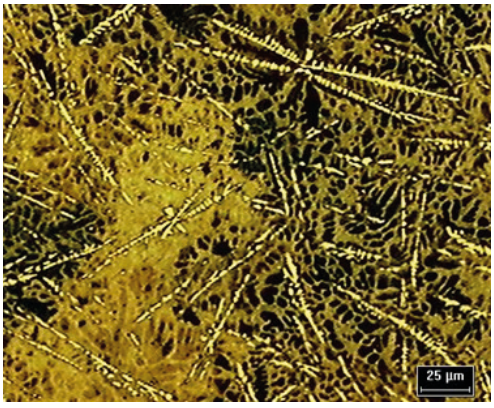

Fig. 6c Bottom of the sample (Tf)

Fig. 6 Photomicrographs of 4.5Cu alloy, CTI, 200x

When verifying the chemical composition throughout the sample, it was found that it does not present considerable gradients, therefore it is possible to consider that a non-homogeneous microstructure will be obtained, with notable variations in morphology and phase distribution if speeds are not reached. uniform cooling rates throughout the volume of a cast part. This approach coincides with what was obtained in a previous work (Ma, 2000) in which using the Bridgman technique, where the growth speed of the primary phase is precisely controlled, it is concluded that by varying the growth speed different results are obtained. morphologies and solid fraction of the primary ε phase and its interrelation with the η phase peritectic is modified. In none of these studies does the phase composition

change, except in those samples with a chemical composition close to the formation limit of the primary phase in which it fails to form when a notable increase in the cooling rate occurs (Rashid, 1991; Jareño et al, 2010; Jareño, 2010).

Fig. 7 shows a photomicrograph taken from the lower edge of the 3.8Cu alloy sample after being subjected to the CTII thermal cycle. In the photomicrograph in Fig. 7a, the upper part corresponds to the surface where contact with water began at 7 °C. In the area close to the surface, a high concentration of ε phase with a spheroidal morphology is observed and as the distance to the solidification front increases, not only the morphology, but also the distribution of this phase and its interrelationship with the η phase peritectic, as seen in Figs. 6 and 7b. In the case of solidification using the Bridgman technique (Ma, 2000), the solidification front is fixed and the sample with a diameter of 1.1 mm or 2.5 mm moves relative to it at a constant speed. This way, a uniform microstructure is achieved with an increase in the formation of the primary phase ε as the growth speed increases for the same Cu content since a tempering effect is produced between the liquid metal and the front. of solidification throughout the entire length of the sample. This behavior is different from that obtained when solidifying the samples at cooling rates between 0.4 °C/s and 18 °C/s in which the fraction of ε decreases with the increase in the cooling rate in this speed range. (Jareño et al, 2010: Jareño, 2010). If we look at the photomicrographs in Figs. 6 and 7a, it is possible to see that the thermal shock that occurs during quenching between the water at 7 °C and the liquid metal close to the solidification front produces a notable difference in the formation and morphology of the primary phase ε in this area. of the sample, and therefore in its interrelation with the η phase peritectic, in comparison with the liquid that cools at different speeds in the areas far from this interface.

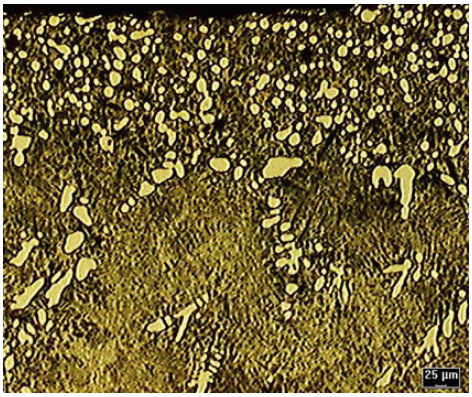

Fig. 7a Photomicrograph at 50 x

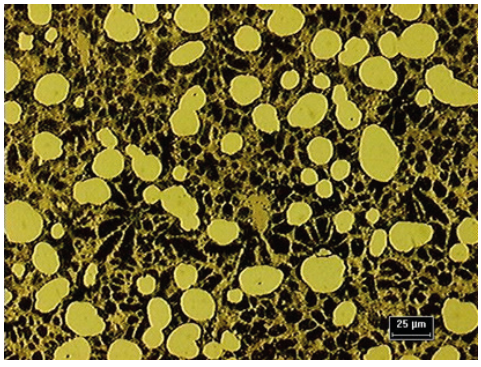

Fig. 7b Sector of Fig. 7 a near the surface at 500 x

Fig. 7 3.8Cu alloy, Photomicrograph of the surface in contact with the solidification front

The spheroidization of the epsilon phase observed in Fig. 7b is related to the permanence at the end temperature of the primary reaction, the point of dendritic coherence, and it is possible to obtain it in these alloys with isothermal permanence in the temperature range between the primary reaction temperature and the formation temperature of the secondary phase eta (Jareño, 2010).

On the other hand, by applying the CTIII thermal cycle, it is possible to obtain a more uniform microstructure throughout the entire volume of the sample, Fig. 8.

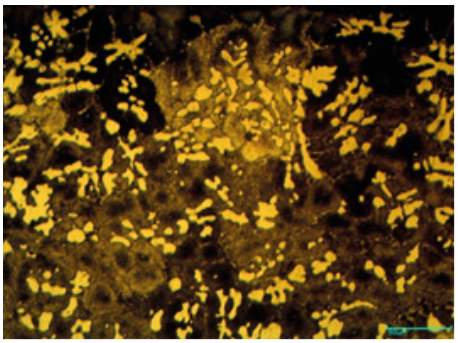

Fig. 8a Zone a, top of the sample

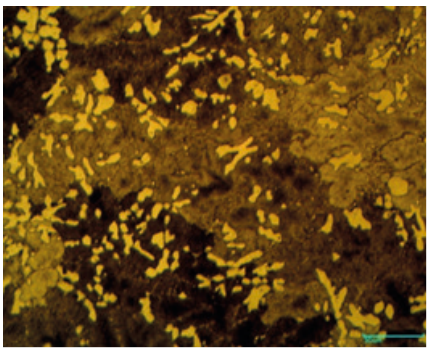

Fig. 8b Zone m, sample mean

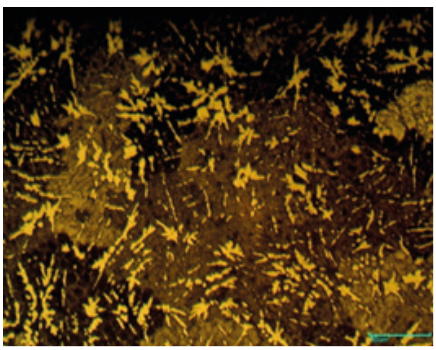

Fig. 8c, Zone s, in contact with the cooled surface, solidification front.

Fig. 8 ACuZinc5 alloy. Thermal Cycle CTIII, scale: 50 µm, 200x.

According to Fig. 8, the distribution and morphology of the primary phase obtained as a result of stirring in the CTIII thermal cycle allows the microstructure to be modified in a notable way since greater microstructural homogeneity is produced in terms of the size of the primary phase, to the morphology and distribution of the phases. However, the morphological differences of the ε phase in the microstructure of the s zone with respect to the m and a zones are noticeable. In the s zone, fine dendrites are observed dispersed among other larger dendritic formations. The persistence of fine dendrites in the s zone may be related to a higher cooling rate compared to the m and a zones, and due to insufficient permanence and deformation rate. According to Fleming et al. (1991), with the increase in the deformation speed, greater spheroidization of the primary phase is achieved and greater permanence allows dendritic thickening (Stefanescu, 2009, Jareño et al., 2012). On the other hand, taking into account the patent by Aoyama et al. (2006), it must be controlled that the combination of deformation speed and permanence does not promote the formation of a rosette or globular structure of the primary phase with an average size outside the appropriate range for injection in a semi-solid state, which is between 30 and 50 µm.

CONCLUSIONS

The sequence and solidification conditions significantly affect the formation and growth of the primary phase ε in Zn(3-4)Al(3.8-5.6)Cu alloys. To the extent that the cooling rate of one area of a piece varies with respect to another, a notable change occurs in the morphology and fraction of this phase, and as a consequence in the interrelationship with the η phase. Therefore, in the case of parts cast in molds with a high temperature gradient between the liquid metal and the mold wall, it is unlikely that a uniform microstructure will be obtained. However, in injection processes at high pressures it is possible to improve the mechanical properties of these alloys due to a better interrelation between the ε and η phases (Rashid 1991; Hanna, 1997), which could be related to the formation of sufficient ε phase. and fine due to the effect of the thermal shock of the liquid metal with the walls of the mold

and the distribution of this phase in the metal bath as a nucleation substrate resulting from the fluid dynamics associated with filling the mold, characteristic of these casting processes. On the other hand, the application of thermal and stirring cycles during the solidification of these alloys significantly modify the morphology and distribution of the primary epsilon phase.

REFERENCES

Aoyama S., Liu C., Sakazawa T., Pan Y., 2006. Method of producing semi-solid metal slurries. US Patent No 7,051,784 B2.

Durman M., Murphy S., 1991. Precipitation of metastable ε-phase in a hypereutectic zinc-aluminium alloy containing copper. Acta Metal et Mater., Vol. 39, No. 10, 2235-2242. https://doi.org/10.1016/0956-7151(91)90005-L.

Flemming M.C., 1991. Behavior of Metal Alloys in the Semisolid State. Metall. Trans., Vol. 22A, 957-981. https://doi.org/10.1007/BF02661090

Haughton J.L., Bingham K. E., 1921. The Constitution of the Alloys of Aluminium Copper, and Zinc containing High Percentages of Zinc, Proceedings of the Royal Society of London, Series A, 47-68. DOI: 10.1098/rspa.1921.0022

Hanna M.D., Rashid M.S., 1997. High Strength, High temperature and High Strains Applications of a Zinc based alloys. US Patent No. 5,603,552

Jareño E.D. Tesis Doctoral, Estudio del efecto del cobre, del aluminio y de la velocidad de enfriamiento en la secuencia de solidificación de aleaciones Zn-Al-Cu. Cinvestav, Unidad Ramos Arizpe (2010)

Jareño E.D., Castro M.J., Maldonado S.I., Hernández F.A., 2010. The effects of Cu and cooling rate on the fraction and distribution of epsilon phase in Zn–4Al–(3–5.6)Cu alloys. J. of All and Comp., Vol. 490, 524-530. https://doi.org/10.1016/j.jallcom.2009.10.073

Jareño E.D., Maldonado S.I., Hernández F. A., 2012. Efecto de las condiciones de enfriamiento sobre la fracción y morfología de la fase primaria épsilon en una aleación comercial ACuZinc5. Rev. Metal M 48 (6), 414-423. DOI: 10.3989/revmetalm.1163

Lashkari O., Ghomashchi R., 2007. The implication of rheology in semi-solid metal processes: An overview. J. of Mat. Proc. Tech., Vol. 182, 229-240. DOI: 10.1016/j.jmatprotec.2006.08.003.

Ma D., Li Y., NG S.C., Jones H., 2000. Unidirectional solidification of Zn-rich Zn-Cu peritectic alloys-II. Length scales. Acta mater., Vol. 48, 1741-1751. https://doi.org/10.1016/S1359-6454(00)00003-3

Rashid M.S., Hanna M.D., 1991. Creep resistant die cast zinc alloy, US Patent No. 4,990,310